A Simple Method to Design Wide-Band Electronically Tunable Combline Filters

Germán Torregrosa-Penalva, *Student Member, IEEE*, Gustavo López-Risueño, *Student Member, IEEE*, and José I. Alonso, *Member, IEEE*

***Abstract*—A new systematic approach for designing wide-band tunable combline filters is presented. New results on tunable combline filter theory are proposed and explicit design formulas, to obtain the filter design parameters from specifications, are included. These design parameters are: center frequency, resonator electrical length, *instantaneous* bandwidth, and tuning capacitance. The proposed design technique is used to construct an X-band wide-band microstrip tunable filter from 8 to 12 GHz with commercial GaAs FETs as tuning elements. Parasitic effects and simulation problems are also discussed.**

***Index Terms*—Combline filters, electronically tunable filters, frequency control.**

I. Introduction

COMBLINE filters are broadly used as bandpass filters in modern microwave and millimeter-wave subsystems due to their compactness, excellent stopband and selectivity performance, and ease of integration [1], [2]. If they are built on a microstrip substrate, very low cost and small size can be achieved, making them very attractive for mobile communication [3] and wide-band radar systems [4]. On the other hand, the need of flexibility in commercial and military radio-frequency applications demands the use of high-performance electronically tunable filters with high tuning speed, high-Q factor, and broad tuning range [5].

Microstrip combline and interdigital tunable filters have been described by many authors. Hunter and Rhodes [6] describe a method to design combline filters. Although they provide basic expressions and useful results, their approach is neither suitable for microstrip technology, nor gives the criteria to choose the filter design parameters. In [7] and [8], a varactor-tunable high-Q microwave filter is presented where the tuning element losses are compensated by the use of an FET circuit. However, this approach is not feasible for wide tuning ranges. The advantages and drawbacks of using either varactor diodes or MESFET varactors to tune the passband center frequency are discussed in [9], along with a review of end-coupled microstrip-line bandpass filters. More recently, in [10], a varactor electronically tunable interdigital filter is shown. Parasitic effects of the varactor series resistance and the resonator electrical length on the overall resonator Q factor and filter insertion losses are also discussed in detail.

However, these papers do not provide systematic and consistent criteria to establish the filter design parameters straightforward from the initial specifications. We present a simple method to design tunable combline filters systematically from the specifications so that broad tuning ranges can be achieved. The method is applied to microstrip combline filters with tapped-line inputs. Its fundamentals are described in Section II and an illustrative design example is shown in Section III. Section IV includes simulations, measurements, and comments on the most important nonideal effects encountered in the practical implementation of the filter. This is a five-pole filter with a tuning range from 8 to 12 GHz. The measured *instantaneous* bandwidth range varies from 630 to 1350 MHz. Commercial GaAs FETs in a *cold* configuration are used as tuning devices.

II. Tunable Combline Filters Design Procedure

The design method of tunable filters suggested in this paper can be split into two steps. The first step consists of the suitable selection of the design parameters required to undertake the second step. These are: 1) design center frequency (f_0); 2) resonator electrical length (θ_0) at f_0; 3) *instantaneous* bandwidth (ΔB_{L0}); and 4) tuning device capacitance (C_{s0}) at f_0. The second step comprises the design of a microstrip tapped-line combline filter with a fixed center frequency making use of the method in [11]. This method assumes a quasi-TEM approximation and negligible nonadjacent-line coupling, and uses the equivalent circuit by Cristal [12]. Although its inaccuracy has been proven [13], it provides good agreement in and near the filter passband, and can be used for design purposes. The characteristic admittances of the coupled-line structure can then be obtained using the expressions proposed in [14]. The filter physical dimensions can be calculated using synthesis formulas.

The necessary criteria for determining the above-mentioned parameters (f_0, θ_0, ΔB_{L0}, and C_{S0}) from the specifications constitute the main contribution of this paper and are explained in Sections II-A–II-D. The most common specifications that a tunable filter must meet are as follows:

Manuscript received September 20, 2000; revised February 2, 2001. This work was supported by INDRA DTD under Contract P96093259 and by The National Board of Scientific and Technology Research, Comisión Interministerial de Ciencia y Tecnología under Project TIC-99-1172-C02-01.

The authors are with the Grupo de Microondas y Radar, Departamento de Señales, Sistemas y Radiocomunicaciones, Universidad Politécnica de Madrid, Madrid, Spain (e-mail: ignacio@gmr.ssr.upm.es).

Publisher Item Identifier S 0018-9480(02)00023-6.

- tuning range or tuning bandwidth ($[f_1, f_2]$): the range of frequencies in which the filter should be tuned;
- *instantaneous* bandwidth[1] range ($[\Delta B_{L\min}, \Delta B_{L\max}]$) the filter has within the tuning range, given for a particular attenuation level (L dB);
- maximum reflection coefficient (L_r) in the filter passband;
- filter-selectivity requirements; specified, for example, at a percentage of the filter passband edge frequencies;
- capacitance range ($[C_{s\min}, C_{s\max}]$) of the tunable elements used.

A. Design Center Frequency f_0

Due to the fact that rejection requirements are harder to attain at lower tuning frequencies,[2] the frequency f_0 is selected to be

$$f_0 = \sqrt{f_1 \cdot f_2} \tag{1}$$

where f_1 and f_2 are the tuning bandwidth lower and upper limits. A smaller value of f_0 may be chosen on the assumption that requirements at the highest part of the tuning range will be met without problems. In any case, (1) will be used in the design procedure.

B. Electrical Length θ_0

Hunter and Rhodes [6] propose a three-step transformation of the filter equivalent circuit consisting of: 1) the admittance inverter equivalent circuit of the filter (see [6, Fig. 4]); 2) scaling the network admittances by $\tan(\theta)/\tan(\theta_0)$; and 3) transforming the previous network to the low-pass prototype with admittance inverters by the inverse of a bandpass transformation. Assuming a narrow *instantaneous* bandwidth, it follows that

$$\Delta B_L = k\frac{\theta \cdot \tan(\theta)}{\tan(\theta) + \theta \cdot \left(1 + \tan^2(\theta)\right)}. \tag{2}$$

Equation (2) shows the filter *instantaneous* bandwidth dependence on the resonator electrical length θ at the tuning frequency. k is a constant that depends on the resonator geometry. If k is removed, the logarithm of the normalized *instantaneous* bandwidth ΔB_{Ln} can be defined as follows:

$$\begin{aligned}\Gamma =& 10\log_{10}(\Delta B_{Ln}) \\ =& 10\log_{10}\left(\frac{\theta \cdot \tan(\theta)}{\tan(\theta) + \theta \cdot \left(1 + \tan^2(\theta)\right)}\right).\end{aligned} \tag{3}$$

Equation (3) is depicted in Fig. 1. Due to the linear relationship between electrical length and frequency, this equation also shows the *instantaneous* bandwidth dependence on the tuning frequency. Since a typical specification consists of maintaining the *instantaneous* bandwidth within a range, $[\Delta B_{L\min}, \Delta B_{L\max}]$, (3) is very useful to select θ_0. As the maximum of this equation is reached when $\theta_{\max} \approx 53°$, it can be assigned $\theta_{\max}$ to $\Delta B_{L\max}$ so that the maximum tuning range is attained fulfilling the bandwidth requirement, as illustrated in Fig. 1.

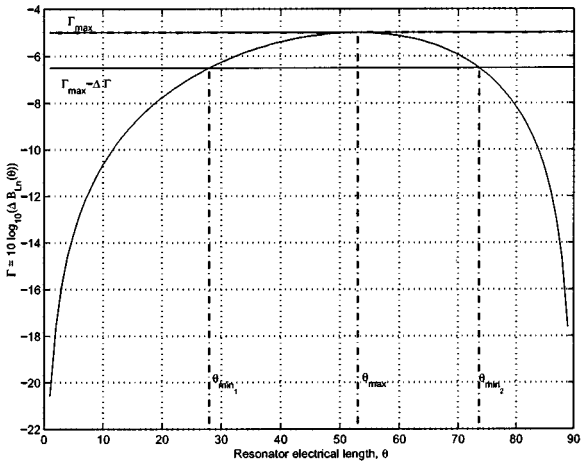

Fig. 1. Normalized instantaneous bandwidth $\Gamma = 10\log_{10}(\Delta B_{Ln})$. $\theta_{\max}$ is the electrical length where Γ reaches its maximum value. Once $\Delta\Gamma$ is known, $\theta_{\min_1}$ and $\theta_{\min_2}$ can be obtained.

If

$$\Delta\Gamma = 10\log_{10}\frac{\Delta B_{L\max}}{\Delta B_{L\min}} \tag{4}$$

and

$$\theta_{\min_1}, \theta_{\min_2} = \Gamma^{-1}\left(\Gamma(\theta_{\max}) - \Delta\Gamma\right) \tag{5}$$

then the filter must satisfy

$$\theta_{\min_1} \le \theta_1 \le \theta_0 \le \theta_2 \le \theta_{\min_2} \tag{6}$$

where θ_1 and θ_2 are, respectively, the resonator electrical length at f_1 and f_2. Constraint (6) can be written as follows:

$$\theta_{\min_1}\frac{f_0}{f_1} \le \theta_0 \le \theta_{\min_2}\frac{f_0}{f_2}. \tag{7}$$

From (7), a range of possible θ_0 values can be obtained to satisfy the specified tuning range.

C. Instantaneous Bandwidth ΔB_{L0}

The *instantaneous* bandwidth ΔB_{L0} (for L dB attenuation) at f_0 is computed as it is done with θ_0. Using the relationship

$$\begin{aligned}k =& \frac{\min_{\theta\in\{\theta_1,\theta_2\}}\left(\Delta B_L(\theta)\right)}{\min_{\theta\in\{\theta_1,\theta_2\}}\left(\Delta B_{Ln}(\theta)\right)} \\ =& \frac{\Delta B_L(\theta_0)}{\Delta B_{Ln}(\theta_0)} = \frac{\Delta B_L(\theta_{\max})}{\Delta B_{Ln}(\theta_{\max})}\end{aligned} \tag{8}$$

and the *instantaneous* bandwidth specification, an expression similar to the θ_0 constraint is obtained for ΔB_{L0} as follows:

$$\begin{aligned}\frac{\Delta B_{L\min}}{\min_{\theta\in\{\theta_1,\theta_2\}}\left(\Delta B_{Ln}(\theta)\right)}\Delta B_{Ln}(\theta_0) \\ \le \Delta B_{L0} \le \frac{\Delta B_{L\max}}{\Delta B_{Ln}(\theta_{\max})}\Delta B_{Ln}(\theta_0).\end{aligned} \tag{9}$$

Once ΔB_{L0} is known and the filter order is selected to meet the selectivity requirements, the Chebyshev approximation parameters can be computed through the conventional low-pass

[1] *Instantaneous* means in a specific tuning frequency within the range of tunable frequencies.

[2] Due to the tuning element low-Q factor at those low tuning frequencies [10].

to bandpass transformation and the Chebyshev approximation [15].

D. Capacitance C_{s0}

The equation that relates a tuning frequency and its corresponding tuning capacitance is [6]

$$\frac{1}{Y_a}\cdot 2\pi f\cdot\tan(\theta)\cdot C_s(f)=1 \tag{10}$$

where θ is the resonator electrical length at the tuning frequency f, Y_a is the resonator characteristic admittance, and $C_s(f)$ is the tuning capacitance that tunes the filter at f. Varactors and FET's in *cold* configuration are usually used as tuning elements.

The tuning device provides a variable capacitance within a range $[C_{s\min}, C_{s\max}]$. According to (10), the smallest capacitance tunes the highest tunable frequency, f_{Mtun}, and the largest capacitance the lowest one, f_{mtun}. Additionally, the maximum tunable frequency can be expressed as an implicit function of C_{s0} by means of

$$f_{\mathrm{Mtun}}\,C_{s\min}\tan\left(\frac{\theta_0}{f_0}f_{\mathrm{Mtun}}\right)=f_0C_{s0}\tan(\theta_0) \tag{11}$$

and the minimum tunable frequency by

$$f_{\mathrm{mtun}}C_{s\max}\tan\left(\frac{\theta_0}{f_0}f_{\mathrm{mtun}}\right)=f_0\,C_{s0}\tan(\theta_0). \tag{12}$$

As can be noticed, the lower C_{s0} is, the lower f_{mtun} and f_{Mtun} are. Defining C_{s0_1} and C_{s0_2} as

$$f_{\mathrm{mtun}}(C_{s0_1})=f_1 \tag{13}$$

$$f_{\mathrm{Mtun}}(C_{s0_2})=f_2 \tag{14}$$

the following constraint is obtained:

$$C_{s0_2}\le C_{s0}\le C_{s0_1}. \tag{15}$$

Therefore, the range of possible C_{s0} values is given by

$$\frac{f_2\tan\left(\frac{\theta_0\cdot f_2}{f_0}\right)}{f_0\tan(\theta_0)}C_{s\min}\le C_{s0}\le\frac{f_1\tan\left(\frac{\theta_0\cdot f_1}{f_0}\right)}{f_0\tan(\theta_0)}C_{s\max}. \tag{16}$$

To illustrate the previous discussion, the reader may refer to Fig. 2, where the following parameters have been selected: tuning bandwidth $=[8,12]$ GHz, capacitance range $=[0.18,0.6]$ pF, $f_0=9.8$ GHz, and $\theta_0=50°$. In Fig. 2, the variation with the capacitance C_{s0} of the lowest and highest tuning frequencies, i.e., f_{mtun} and f_{Mtun}, respectively, is shown. The capacitances C_{s1} and C_{s2} are also depicted. In this case, the range of C_{s0} possible values results in $[0.337,0.357]$ pF.

III. Filter Design Example

In this section, a specific design of an electronically tunable combline filter will be performed following the previously described technique. The proposed filter schematic is shown in Fig. 3.

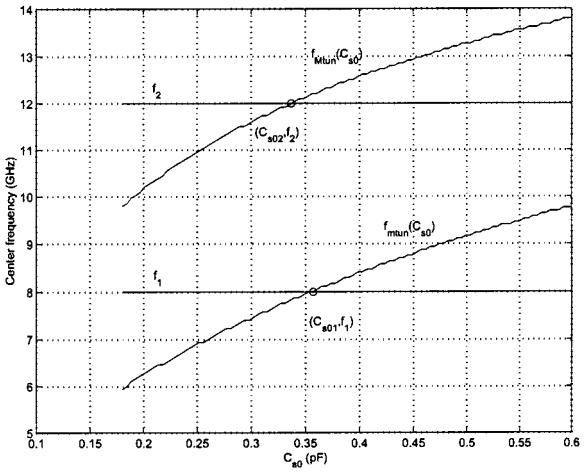

Fig. 2. Illustrative example of the C_{s0} selection. The dependence of f_{Mtun} and f_{mtun} on C_{s0} is shown. C_{s0} must be selected so that $f_{\mathrm{Mtun}}\ge f_2$ and $f_{\mathrm{mtun}}\le f_1$ in order to achieve the desired tuning range.

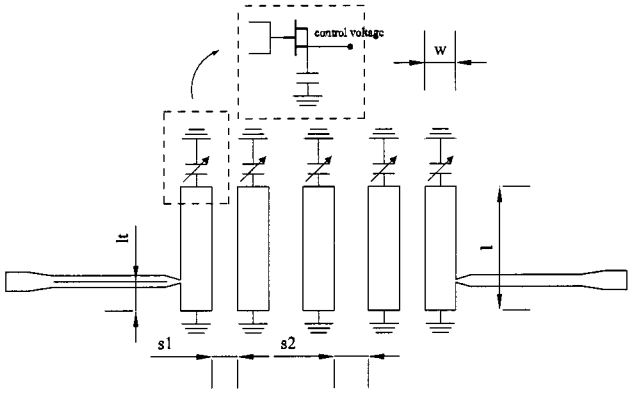

Fig. 3. Designed filter schematic.

TABLE I
DESIGN SPECIFICATIONS

f_1	8.0 GHz
f_2	12.0 GHz
ΔB_{Lmin}	600 MHz ($L=1.5$ dB)
ΔB_{Lmax}	1000 MHz ($L=1.5$ dB)
Rejection at $f_{c1}-0.1f_{c1}$	15.0 dB
Rejection at $f_{c2}+0.1f_{c2}$	15.0 dB
$[C_{smin}, C_{smax}]$	$[0.18, 0.6]$ pF
L_r	-10.0 dB

A. Filter Requirements and Specifications

The initial design requirements and specifications are given in Table I, where f_{c1} and f_{c2} are the cutoff frequencies at $L=1.5$ dB. As a tuning device, the NE71000 MESFET by NEC in a *cold* configuration is employed. Its characterization is described in the Appendix.

B. Design Parameters

The systematic design approach provided in Section II is next applied. First, from (1), the design center frequency f_0 is determined. Next, making use of (7), the resonators electrical length θ_0 is obtained. Once the previous parameters are determined, the *instantaneous* bandwidth ΔB_{L0} is calculated using (9) and,

TABLE II
FILTER DESIGN PARAMETERS

f_0	9.79 GHz, $8.0 \leq f_0 \leq 12.0$ GHz
θ_0	$50°$, $28.29° \leq \theta_0 \leq 62.59°$
ΔB_{L0}	775 MHz, $645 \leq \Delta B_{L0} \leq 995$ MHz
C_{s0}	0.35 pF, $0.337 \leq C_{s0} \leq 0.356$
N	5
L_{ar}	0.1 dB
w	0.072

TABLE III
FILTER PHYSICAL DIMENSIONS

widths (w)	0.400 mm
length (l)	1.590 mm
spacings (s1,s2)	(0.331, 0.439) mm
length from ground to input line (lt)	0.370 mm

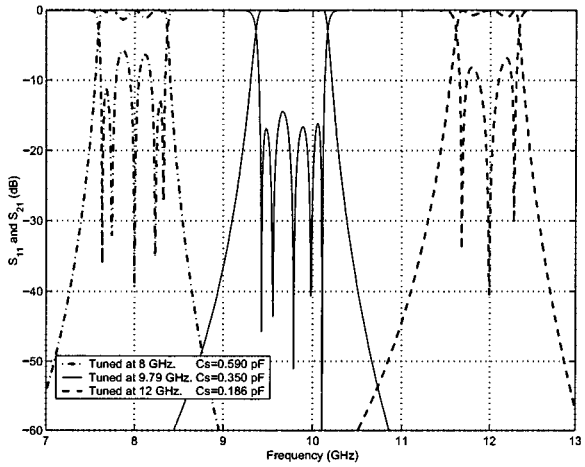

Fig. 4. Ideal filter simulated response.

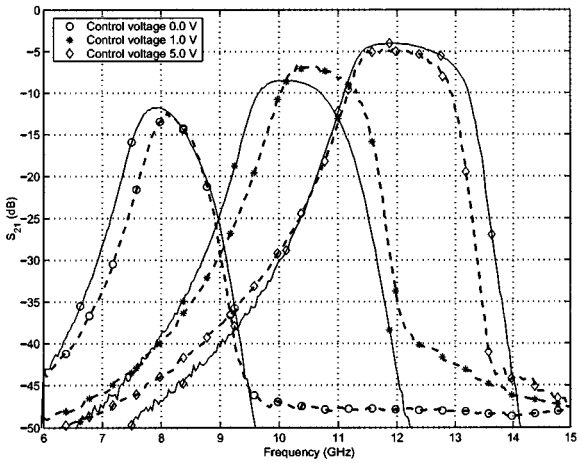

Fig. 5. Insertion losses for various control voltages: simulations (dashed line) and measurements.

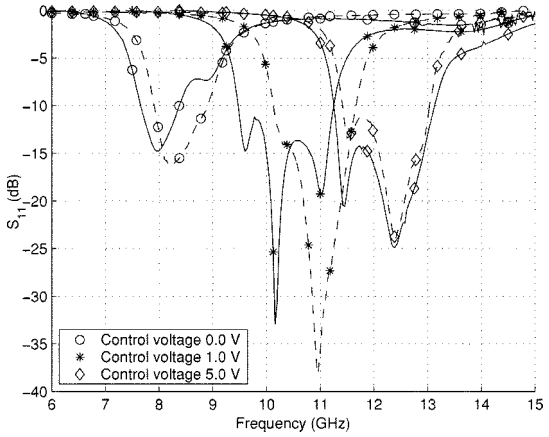

Fig. 6. Return losses for various control voltages: simulations (dashed line) and measurements.

finally, the parameter C_{s0} is obtained using (16). The design parameter values and their variation range obtained through the design technique are shown in Table II along with the Chebyshev approximation parameters.

C. Physical Dimensions

The combline filter physical dimensions are calculated by means of [11] and [14] and synthesis formulas. In our case, Linecalc has been used to synthesize the physical dimensions (see Fig. 3) shown in Table III. The filter has been fabricated on a 254-μm alumina substrate with a dielectric constant of 9.9 and a metal thickness of 10 μm.

IV. SIMULATIONS AND MEASUREMENTS

First, the filter response is simulated making use of the model given in [12] with ideal transmission lines. Capacitors with no parasitic effects are used as tuning elements. The short circuits at the end of the resonators are also assumed to be ideal. This response is shown in Fig. 4. As can be seen, it meets the initial requirements given in Table I, except the return losses specification at the extreme tuning frequencies, which is due to the narrow-band matching behavior of the tapped-line inputs.

Second, parasitic effects must be considered. These effects are: 1) the effects introduced by the low-Q FETs used as tuning elements; 2) the resonators' short circuit's inductive and resistive behavior; and 3) the dispersive characteristics of microstrip transmission lines. The simulated response of the filter is obtained making use of Libra. This simulator does not support a coupling multiple resonator structure, thus, in order to perform the simulations, it is necessary to use the technique described in [16]. Simulations after optimizing with Libra and measurements of the final filter prototype are given in Figs. 5 and 6 for different control voltages . These simulations are performed using: 1) real measurements of the FET (see the Appendix) and 2) an equivalent circuit for the nonideal behavior of the short circuits consisting on an *RL* series circuit.

Taking into account the high design center frequency (9.79 GHz), the good agreement between simulations and measurements should be remarked. The tuning frequency for a given control voltage is predicted with an error smaller than 5%. The discrepancy between the insertion losses' measurements and simulations is always smaller than 2.5 dB. The typical behavior of the insertion losses' reduction with tuning frequency [10] can also be noticed. The discrepancies between measured and simulated *instantaneous* bandwidth are due to

TABLE IV
FILTER MEASURED PERFORMANCE

f_1	8.0 GHz
f_2	12.0 GHz
ΔB_{Lmin}	610 MHz ($L = 1.5$ dB)
ΔB_{Lmax}	1380 MHz ($L = 1.5$ dB)
Rejection at $f_{c1} - 0.1f_{c1}$	> 15.0 dB
Rejection at $f_{c2} + 0.1f_{c2}$	> 15.0 dB
$[C_{smin}, C_{smax}]$	$[0.18, 0.6]$ pF
L_r	< -10.0 dB

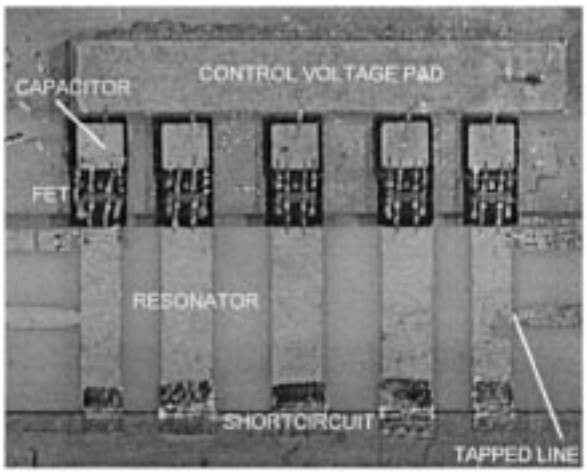

Fig. 7. Filter protoype.

TABLE V
NOISE FIGURE, INPUT P1 dB, AND INPUT IP3

Control Voltage (V)	NF (dB)	Input P1dB (dBm)	Input IP3 (dBm)
0.5	13.0	8.0	18.5
5	4.5	21.0	29.0

the differences between the FETs' characteristics—they come from different batches—and to the simulator models (see [16] for a comparison of different computer-aided design (CAD) tools). Table IV resumes the performance of the filter response shown in Figs. 5 and 6.

Fig. 7 is a photograph of the filter prototype.

In order to fully characterize the designed filter, other important parameters are also measured. The tuning time is measured to be smaller than 25 ns at 25 °C. The measured noise figure, 1-dB compression point (P1 dB) and third-order intermodulation intercept point (IP3) are given in Table V for different control voltages.

The IP3 is measured making use of two tones 200 MHz apart. The third-order mixing products are within the filter 1.5-dB *instantaneous* bandwidth. The small values of measured P1 dB and IP3 at low control voltages are due to the fact that the FET's gate diode starts conducting with smaller signal levels.

V. CONCLUSIONS

A novel and easy to apply systematic procedure to design tunable combline filters has been presented in this paper. The proposed method sets the range of values of the key parameters necessary to design this kind of tunable filters (f_0, θ_0, ΔB_{L0}, C_{s0}) and allows the achievement of broad tuning ranges. The method has proven to be extremely useful in the design of an X-band FET electronically tunable microstrip combline filter. Additionally, a discussion on the most relevant nonideal effects has also been presented.

TABLE VI
FET EQUIVALENT CIRCUIT

Control Voltage (V)	R_{eq} (Ω)	C_{eq} (pF)	L_{eq} (nH)
0	2.8	0.40	0.23
1	2.16	0.21	0.23
5	1.78	0.15	0.23

APPENDIX
TUNING ELEMENTS—CHARACTERIZATION AND MEASUREMENTS

One of the key elements in designing a wide-band tunable combline filter is the selection of the tuning element. In the case of this paper, a GaAs FET in a *cold* configuration (see Fig. 3) is chosen (NE71000 by NEC), although other elements were also proven to be suitable for this kind of designs. The characterization of these tuning devices is essential if the range of available capacitance values needs to be accurately determined. From the S_{11} parameter measurement of the *cold*-FET, it is noticed that a simple *RLC* series circuit is accurate enough to model its behavior. Table VI gives the *RLC* series equivalent-circuit values for the FET used as a tuning element for different control voltages, where $R_{\rm eq}$, $C_{\rm eq}$, and $L_{\rm eq}$ come basically from the gate resistance, gate–drain and gate–source parallel capacitance, and the bonding-wire inductance.

In order to account for the bonding-wire inductance effect on the reactance that loads the resonators, it is necessary to define an effective capacitance that is used to determine $[C_{s\,\rm min}, C_{s\,\rm max}]$ as given in the following:

$$\frac{1}{2\pi f_1 C_{\rm eq}} - 2\pi f_1 L_{\rm eq}\bigg|_{V_{\rm control}=0\ \rm V} = \frac{1}{2\pi f_1 C_{s\,\rm max}} \tag{17}$$

$$\frac{1}{2\pi f_2 C_{\rm eq}} - 2\pi f_2 L_{\rm eq}\bigg|_{V_{\rm control}=5\ \rm V} = \frac{1}{2\pi f_2 C_{s\,\rm min}}. \tag{18}$$

REFERENCES

[1] G. L. Hey-Shipton, "Combline filters for microwave and millimeter-wave frequencies: Part 1," Watkins–Johnson Company, Tech. Notes, vol. 17, Sept./Oct. 1990.
[2] G. L. Matthaei, "Comb-line band-pass filters of narrow or moderate bandwidth," *Microwave J.*, pp. 82–91, Aug. 1963.
[3] P. Alinikula and R. Kaunisto, "Microwave active filters for wireless applications: Systems approach," in *27th European Microwave Conf.*, vol. 1, 1997, pp. 409–414.
[4] D. Fisher and I. Bahl, Eds., *Gallium Arsenide IC Applications Handbook*. New York: Academic, 1995, vol. 1.
[5] C. B. Hofman and A. R. Baron, "Wideband ESM receiving systems—Part II," *Microwave J.*, vol. 24, pp. 57–61, Feb. 1981.
[6] I. C. Hunter and J. D. Rhodes, "Electronically tunable microwave bandpass filters," *IEEE Trans. Microwave Theory Tech.*, vol. MTT-30, pp. 1354–1360, Sept. 1982.

[7] A. Presser, "Varactor-tunable, high-Q microwave filter," *RCA Rev.*, vol. 42, pp. 691–705, Dec. 1981.
[8] S. R. Chandler, I. C. Hunter, and J. G. Gardiner, "Active varactor tunable bandpass filters," *IEEE Microwave Guided Wave Lett.*, vol. 3, pp. 70–71, Mar. 1993.
[9] J. Lin, C.-Y. Chang, Y. Yamamoto, and T. Itoh, "Progress of a tunable active bandpass filter," *Ann. Telecommun.*, vol. 47, no. 11–12, pp. 499–507, 1992.
[10] A. R. Brown and G. M. Rebeiz, "A varactor-tuned RF filter," *IEEE Trans. Microwave Theory Tech.*, vol. 48, pp. 1157–1160, July 2000.
[11] S. Caspi and J. Adelman, "Design of combline and interdigital filters with tapped-line input," *IEEE Trans. Microwave Theory Tech.*, vol. 36, pp. 759–763, Apr. 1988.
[12] E. G. Cristal, "Tapped-line coupled transmission lines with applications to interdigital and combline filters," *IEEE Trans. Microwave Theory Tech.*, vol. MTT-23, pp. 1007–1012, Dec. 1975.
[13] C. Ernst and V. Postoyalko, "Tapped-line interdigital filter equivalent circuits," in *IEEE MTT-S Int. Microwave Symp. Dig.*, vol. 2, 1997, pp. 801–804.
[14] C. Denig, "Using microwave CAD programs to analyze microstrip interdigital filters," *Microwave J.*, vol. 32, pp. 147–152, Mar. 1989.
[15] G. Matthaei, L. Young, and E. M. T. Jones, *Microwave Filters, Impedance-Matching Networks, and Coupling Structures*. Norwood, MA: Artech House, 1980.
[16] G. López-Risueño and J. I. Alonso, "Simulation of interdigitated structures using two-coupled-line models," *Microwave J.*, vol. 43, pp. 70–82, June 2000.

Germán Torregrosa-Penalva (S'99) was born in Novelda, Alicante, Spain, in 1976. He received the Ingeniero de Telecomunicación degree from the Universidad Politécnica de Madrid, Madrid, Spain, in 1999, and is currently working toward the Ph.D. degree at the Universidad Politécnica de Madrid.

He is currently with the Departamento de Señales, Sistemas y Radiocomunicaciones, E.T.S.I. Telecomunicación, Universidad Politécnica de Madrid. His research activities are in the area of high-frequency circuit design and radar systems.

Gustavo López-Risueño (S'99) was born in Barcelona, Spain, in 1974. He received the Ingeniero de Telecomunicación degree from the Universidad Politécnica de Madrid, Madrid, Spain, in 1998, and is currently working toward the Ph.D. degree at the Universidad Politécnica de Madrid.

He is currently with the Departamento de Señales, Sistemas y Radiocomunicaciones, E.T.S.I. Telecomunicación, Universidad Politécnica de Madrid. His research activities are in the area of radar signal processing and high-frequency circuit design.

José I. Alonso (M'90) was born in Villacañas, Toledo, Spain. He received the Ingeniero de Telecomunicación and Ph.D. degrees from the Universidad Politécnica de Madrid, Madrid, Spain, in 1982 and 1989, respectively.

From 1982 to 1985, he was a Microwave Design Engineer at Telettra España S.A. (now Alcatel Standard S.A.). In 1985, he joined the Departamento de Señales, Sistemas y Radiocomunicaciones, E.T.S.I. Telecomunicación, Universidad Politécnica de Madrid, where he is currently a Professor. He has taught courses on microwave circuit design, electrical networks and filter theory, test and measurements of microwave circuits, and laboratories related with analog and digital communication systems. He has developed his research with the Grupo de Microondas y Radar in the areas of analysis and simulation of high-speed/high-frequency integrated circuits and their interconnections, computer-aided design, and measurements of hybrid and GaAs monolithic microwave integrated circuits (MMICs), and their applications in the development and implementation of mobile, satellite, optical-fiber communication, and adaptive antenna systems. He is currently involved in the development of circuits and subsystems for the local multipoint distribution system (LMDS).